POLITECNICO DI TORINO
Repository ISTITUZIONALE

PLA conductive filament for 3D printed smart sensing applications

Terms of use:

(Article begins on next page)

20 March 2024

PLA conductive filament for 3D printed smart sensing applications

SCHOLARONE™
Manuscripts

PLA conductive filament for 3D printed smart sensing applications

Abstract

Purpose - This paper presents a study on a commercial conductive PLA filament and its potential application in a 3D printed smart cap embedding a resistive temperature sensor made of this material. The final aim of this study is to add a fundamental block to the electrical characterization of printed conductive polymers, which are promising to mimic the electrical performance of metals and semiconductors. The studied PLA filament demonstrates not only to be suitable for a simple 3D printed concept, but also to show peculiar characteristics that can be exploited to fabricate freeform low cost temperature sensors.

Design/methodology/approach - The first part is focused on the conductive properties of the PLA filament and its temperature dependency. After obtaining a resistance vs temperature characteristic of this material, the same was used to fabricate a part of a 3D printed smart cap.

Findings - An approach to the characterization of the 3D printed conductive polymer has been presented. The major results are related to the definition of resistance vs temperature characteristic of the material. This model was then exploited to design a temperature sensor embedded in a 3D printed smart cap.

Practical implications (if applicable) - This study demonstrates that commercial conductive PLA filaments can be suitable materials for 3D printed low cost temperature sensors or constitutive parts of a 3D printed smart object.

Originality/value – A clear demonstration that a new generation of 3D printed smart objects can already be obtained employing low cost commercial materials.

Keywords

Conductive polymers; PLA; FDM; smart objects

Classification

Research paper;

1. Introduction

Three-dimensional (3D) printing has the potential to revolutionize science and technology in the field of mechanical, electronic and, in general, engineering systems usually manufactured with high-cost facilities, by employing low cost materials and processes and thanks to an easy transfer approach from the idea to the fabrication.

Additive manufacturing is a freeform, easy access bottom up technology and a wide portfolio of low cost printing equipment is currently available on the market, above all Fused Deposition

Modeling (FDM) printers, which are typically applied to prototype fabrication as well as very low volume production (Tyson et al. 2015). This technology surpasses the constraints imposed by the traditional polymer replication (injection moulding and hot embossing) mainly due to the moulds fabrication, thus allowing new design strategies and innovative applications (Milani et al. 2015). Moreover the affordable cost of the consumables brings to very low cost 3D prints. In this framework, the capability to use materials with conductive properties may lead to a new generation of 3D smart devices (Leigh et al. 2012; Lu et al. 2013; Vatani, Engeberg, et al. 2015; Vatani, Lu, et al. 2015; Zhang et al. 2015; Muth et al. 2014; Kong et al. 2014). Employing electrical conductive composites, it is possible to print 3D current supply lines for active or passive elements that are on their own printed by the same materials. This new approach, indeed, provides a novel devices architecture, which on one side surpasses the intrinsic planarity in conventional fabrication and, on the other side, automatically integrates the active components in the structure of the final object leading to a real smart 3D printed system. In this view new commercial polylactic acid (PLA) filaments and FDM represent a benchmark to understand which are the real potentialities of smart objects 3D printing.

The mentioned materials are carbon (Ning et al. 2015) or metal (Mostafa et al. 2009; Nikzad et al. 2011) based composites, in which the polymer matrix is mixed with conductive powders to improve the quality of the printing in terms of mechanical behaviour. In fact, the major interest in these classes of composite is usually about the mechanical improvements as for tensile properties (including tensile strength, Young's modulus, toughness, yield strength, and ductility), flexural properties (including flexural stress, flexural modulus, flexural toughness, and flexural yield strength), fatigue behaviour and so on. A lot of works about the structural and mechanical characterizations can be found, while very few papers are related to the electrical behaviour of such materials (Leigh et al. 2012). In particular intrinsic characteristics, as the variations of electrical properties as a function of external environment, have not been investigated methodically yet.

In this study a PLA conductive filament has been characterized in terms of resistivity versus temperature. Then a resistance vs temperature characteristic of this material was attained and, as a proof of concept, a 3D printed smart cap integrating an electrical contact and a temperature sensor was built.

2. Experimental

2.1 Resistivity measurements approach

Cubic 10x10x10 mm^3 samples made of conductive 2.85 mm diameter PLA filament (Composite PLA - Electrically Conductive Graphite from Protoplant INC) were printed employing a Velleman

K8200 equipped with a 0.5 mm extruder nozzle and with the following settings: an infill density of
60 % (honeycomb rectilinear), an extruder temperature of 225 °C, a bed temperature of 55 °C and
an infill speed of 65 mm/s. A metallic Ti/Al thin layer (thickness: 100 nm for Ti and 700 nm for Al)
was then deposited by sputtering (Kurt Lesker PVD 75) and a physical mask was employed to
obtain circular patterns of 5 mm diameter. A physical shadow mask made of a 0.5 mm thick sheet
of PolyMethylMethAcrylate (PMMA), adherent to the surface, was employed to obtain circular
patterns on the samples. The metal deposition was repeated on the different sides of the samples.
The deposited Ti/Al film provides the optimal electrical contact that is fundamental to achieve
reproducible measurements, moreover the circular patterns are pads with an accurate and defined
dimension allowing to calculate the resistivity of the printed samples. Electrical wires (1 mm
diameter) were bonded on the Ti/Al pads by means of a silver paste (from RS Components). Two
different resistivities (ρ) have been measured (figure 1): the resistivity parallel to the printing table
(ρ_{xy}), and the resistivity along the z axis (ρ_z). ρ was calculated by the following formula (1):

$$\rho = \frac{R \cdot S}{L} \qquad (1)$$

where R is the measured resistance, S is the area of the pad (19.6 mm^2) and L the cube height (10
mm). The resistivity measurements were acquired with the sample loaded in a climatic chamber
(Angelantoni climatic system TY80) with a temperature range between 10°C and 70°C using an
Agilent data logger model 34970A (equipped with the 34901A board). The conductive PLA
filament has a declared resistivity of 115 Ω·cm for the ρ_z and 30 Ω·cm for the ρ_{xy}. During the
measurements, the sample was heated to a specific temperature in the climatic chamber, with an
accuracy of 1 °C $\pm$ 0.1 °C. The samples were tested by increasing and decreasing the temperature
always within the range 10 °C-70 °C, with a step of 10 °C between successive measurements. To
avoid any transitory effect due to material inertia during the experiment, a rest time of 10 min was
imposed for each acquisition at a specific temperature and then the resistance values were acquired
in a 10 minutes window with a sampling rate of 1 sample/minute. Six different samples were tested
with the above mentioned conditions.

2.2 Smart cap design and fabrication

The smart cap was designed using Rhinoceros**®** 3D CAD software and then printed by Object 30
(Stratasys) for the non-conductive parts and by Velleman K8200 for the electric contacts/sensor. As
depicted in figure 2, the cap is composed by: an external cap that contains the contacts and allows
for the sealing to the bottle; a spring that separates the contacts/sensor; the top and bottom
contacts/sensor fixed by a seeger on the bottom of the spring and by a bolt on the top of the cap.
The contacts/sensor were made by the same conductive PLA employed in the previous electrical

characterization, while the other parts were fabricated by VeroWhite Plus FullCure 835 (from Stratasys). The PLA parts were finished by fine abrasive paper, while Object printings were only finished by water jet to remove the supporting sacrificial material. The smart cap fabrication was achieved after several prints to obtain the best joints compromise among the different parts; at the end of this optimisation step the best fabricated smart cap was tested with the same equipment reported previously.

3. Results and discussion

The conductive PLA cubic samples were tested as described in the experimental section and no statistical differences were found between the mean value for the ramp up and ramp down of the temperature. A good reproducibility of the measured values was registered and a statistical standard error of $\pm$ 0.01 Ω was found for $R_{x,y}$ and of $\pm$ 0.15 Ω was found for R_z. The calculated ρ_z and ρ_{xy} for each temperature (table 1-2) show a significant discrepancy from the nominal ones, in particular for the ρ_{xy} that is one order of magnitude smaller. On the contrary, the difference between ρ_z and ρ_{xy} is still significant (about one order of magnitude) as declared by the supplier. Therefore, this difference should be related to how the filament has been fabricated by extruding the original powders; such extruding process probably leads to a filament with a core rich of conductive powder and a shell with a lower concentration of the same.

The most interesting result is the noteworthy variation of resistivity as a function of temperature: 0.1 – 0.85 Ω/°C for $R_{x,y}$ and 0.65 – 5.7 Ω/°C for R_z. It means that it is possible to appreciate a resistance variation as a function of temperature and vice versa to measure the temperature by resistance acquisition. Therefore, it is likely to fabricate a sensor with a sensitivity of about 1 Ω/°C or greater depending on the contacts configurations, along z axis or on the printed layer. The plots in figure 4 show that this dependency is not linear since at higher temperature the resistance variation increases. However it is possible to find the empirical model using a parabolic fit with a R^2 of 0.99:

$$R_z(T) = 0.0532\ T^2 - 0.997\ T + 199.95 \qquad (2)$$
$$R_{x,y}(T) = 0.0071 T^2 - 0.2045\ T + 29.447 \qquad (3)$$

If compared with other commercial thermistors or Pt100 probes, which are based on the well studied Temperature Coefficient of Resistance (TCR) of Pt (Tommasi et al. 2016), similar or higher sensitivity can be attained by choosing a z axis resistance configuration, especially for temperature above 20 °C.

The practical consequence of this behaviour is the possibility to build a 3D printed object where the temperature sensor is not a separated element to be assembled in the structure, but a part of the object itself. To demonstrate this assertion a 3D smart cap has been fabricated. In this system the objective is to determinate the open or close position of the cap by a simple electrical contact, that is by closing the circuit between the 3D printed top and bottom contacts (figure 2 and 3). During the closing and opening of the bottle the resistance has been acquired thus providing both the status (open/close) and the temperature of the cap (figure 5). Such a case study was selected since embodying a very common and critical component in several packaging solutions and commercial goods (food, chemicals, biology, drugs,…), often characterised by customised dimensions and shape depending on the specific use. No particular consideration for future upgrades of the production volume or current regulation (both strictly application dependent) has been taken into account.

This test confirms the hypothesis that a 3D printed object can acquire active features to become more than a simple mechanical component. This also demonstrates that the evolution of 3D printing techniques is closely correlated to the innovation on materials in order to add functionalities and to technologies in order to achieve better resolutions.

4. Conclusion

The presented study focuses on the potentiality of 3D printed conductive polymers, which are a new class of low cost materials that promise to substitute metals and semiconductors, opening the way to a new generation of 3D printed smart objects. After measuring a resistance vs temperature characteristic of this material and defining a simple thermo-electrical model, the same material was used to fabricate a component of a 3D printed smart cap. The results of the conductive PLA thermo-electrical characterization indicate that this material is not only exploitable for its electrical conductivity, but also for its significant variation as a function of temperature. Finally it was demonstrated that it is possible to print a conductive element of a 3D object that is also a temperature sensor. The proof of concept presented in this work has the aim to demonstrate the actual application of functional materials to 3D printing and to inspire new sensors integration solutions, or more generally, new electrical-based functionalities provided to structural components such as: antennas, identification codes, bolometers, UV sensors, magnetic field sensors etc. This opens a new scenario, where for instance personal objects like smartphones, smartwatches, cars, computers, etcetera, but also disposable parts like food packages may be connected each other to provide the right information at right time: for instance by communicating to the shop assistant that

a food is expired or contains allergens, or to inform that the package was exposed to an excess of radiation or, finally to detect any eventual electromagnetic interference between a commercial good and its potential user.

Future investigations will be focused on more complex objects in which the PLA conductive 3D pattern may be employed for both temperature sensing and eventually heating (i.e. anemometric flow sensors) and the miniaturization of the same. Further evolution will cover the integration of the PLA 3D printable material with other Additive Manufacturing technologies to build temperature based sensing solutions integrating all the active features together with a customized 3D printed plastic package.

References

Kong, Y.L. et al., 2014. 3D Printed Quantum Dot Light-Emitting Diodes. *Nano letters*, 14, p.7017−7023.

Leigh, S.J. et al., 2012. A Simple, Low-Cost Conductive Composite Material for 3D Printing of Electronic Sensors. *PLoS ONE*, 7(11), pp.1−6.

Lu, Y., Vatani, M. & Choi, J., 2013. Direct-write / cure conductive polymer nanocomposites for 3D structural electronics. *Journal of Mechanical Science and Technology*, 27(10), pp.2929−2934.

Milani, C. et al., 2015. A hyper-realistic method for facial approximation: the case of the Italian humanist Angelo Poliziano. *Anthropologischer Anzeiger; Bericht über die biologisch-anthropologische Literatur*, 72(2), pp.235−244. Available at: https://www.scopus.com/inward/record.uri?eid=2-s2.0-84942572241&doi=10.1127%2Fanthranz%2F2015%2F0493&partnerID=40&md5=4c4741503778941eab99aed309da28c8.

Mostafa, N. et al., 2009. A Study of Melt Flow Analysis of an ABS-Iron Composite in Fused Deposition Modelling Process. *Tsinghua Science and Technology*, 14(SUPPL. 1), pp.29−37.

Muth, J.T. et al., 2014. Embedded 3D printing of strain sensors within highly stretchable elastomers. *Advanced Materials*, 26(36), pp.6307−6312.

Nikzad, M., Masood, S.H. & Sbarski, I., 2011. Thermo-mechanical properties of a highly filled polymeric composites for Fused Deposition Modeling. *Materials and Design*, 32(6), pp.3448−3456.

Ning, F. et al., 2015. Additive manufacturing of carbon fiber reinforced thermoplastic composites using fused deposition modeling. *Composites Part B: Engineering*, 80, pp.369−378. Available at: http://dx.doi.org/10.1016/j.compositesb.2015.06.013.

Tommasi, A. et al., 2016. Modeling, Fabrication and Testing of a Customizable Micromachined Hotplate for Sensor Applications. *Sensors*, 17(1), p.62. Available at: http://www.mdpi.com/1424-8220/17/1/62.

Tyson, A.L., Hilton, S.T. & Andreae, L.C., 2015. Rapid, simple and inexpensive production of custom 3D printed equipment for large-volume fluorescence microscopy. *International Journal of Pharmaceutics*, 494(2), pp.651−656. Available at:

http://www.ncbi.nlm.nih.gov/pmc/articles/PMC4626572/.

Vatani, M., Lu, Y., et al., 2015. Combined 3D Printing Technologies and Material for Fabrication of Tactile Sensors. *INTERNATIONAL JOURNAL OF PRECISION ENGINEERING AND MANUFACTURING*, 16(7), pp.1375–1383.

Vatani, M., Engeberg, E.D. & Choi, J., 2015. Conformal direct-print of piezoresistive polymer / nanocomposites for compliant multi-layer tactile sensors. *Additive Manufacturing*, 7, pp.73–82. Available at: http://dx.doi.org/10.1016/j.addma.2014.12.009.

Zhang, Y. et al., 2015. Research on electrically conductive acrylate resin filled with silver nanoparticles plating multiwalled carbon nanotubes. *Journal of Reinforced Plastics and Composites*, 34(15), pp.1193–1201. Available at: http://jrp.sagepub.com/cgi/doi/10.1177/0731684415587348.

Table1: $R_{x,y}$ mean value obtained by the measurements and calculated ρ_{xy} values.

Temperature	$R_{x.y}$	ρ_{xy}
(°C)	(Ω)	(Ω·cm)
10	27.66	5.42
20	28.64	5.61
30	29.97	5.87
40	32.72	6.41
50	36.56	7.16
60	41.81	8.20
70	50.28	9.86

Table 2: R_z mean value obtained by the measurements and calculated ρ_z values.

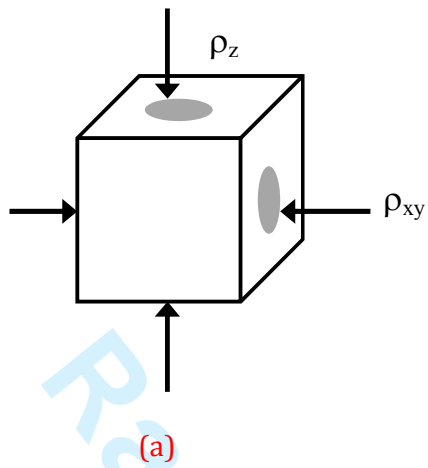| Temperature (°C)	R_z (Ω)	ρ_z ($\Omega \cdot cm$)
10	195.23	38.26
20	201.77	39.55
30	217.33	42.60
40	245.46	48.11
50	281.87	55.25
60	333.33	65.33
70	389.99	76.44

(a)

(b)

Figure 1: schematic of the measurement (a) and a 3D printed sample (b).
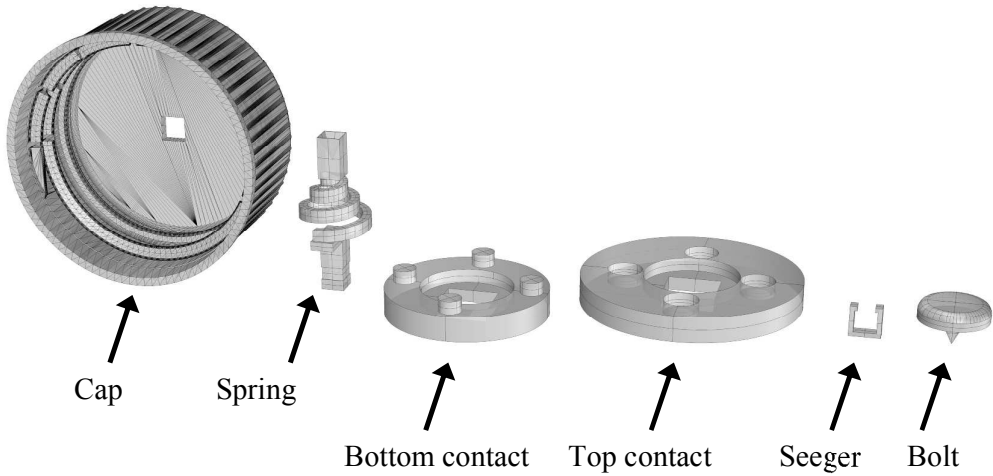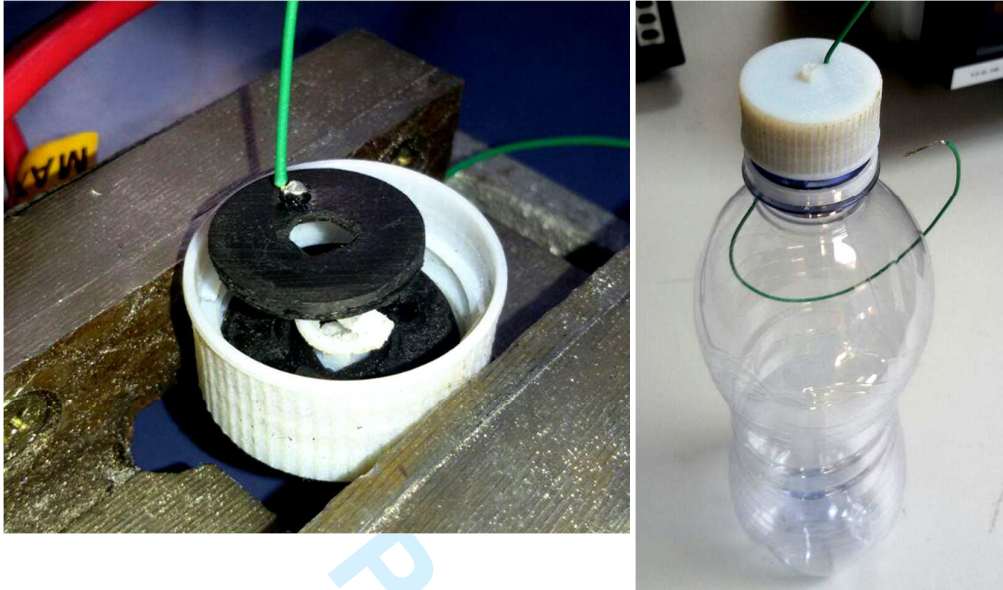
Figure 2: components of the smart cap

Figure 3: Assembled (on the left) and screwed on a bottle (on the right) smart cap.

$$R_z = 0.0532T^2 - 0.997T + 199.95$$
$$R^2 = 0.99982$$

$$R_{xy} = 0.0071T^2 - 0.2045T + 29.447$$
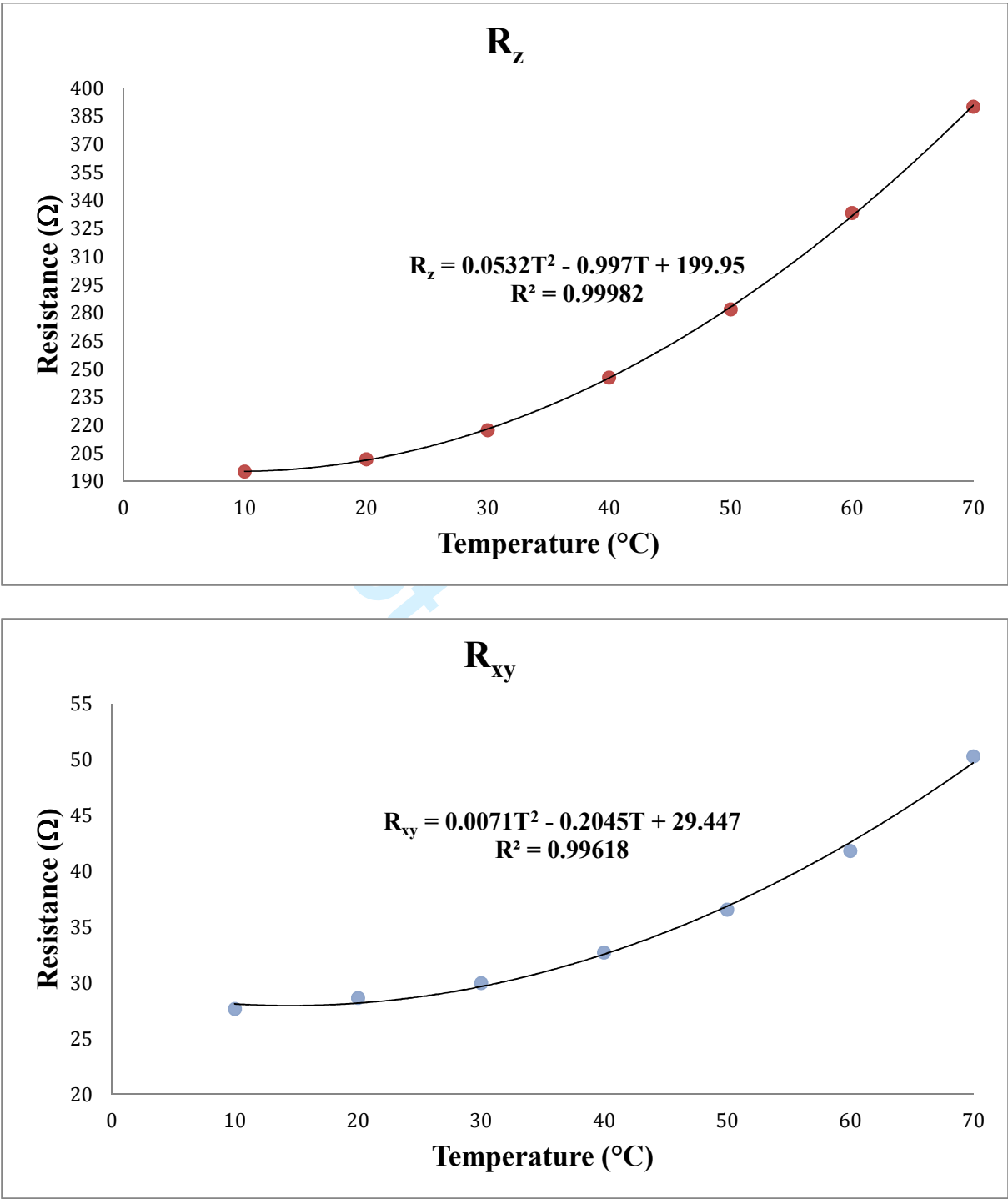$$R^2 = 0.99618$$

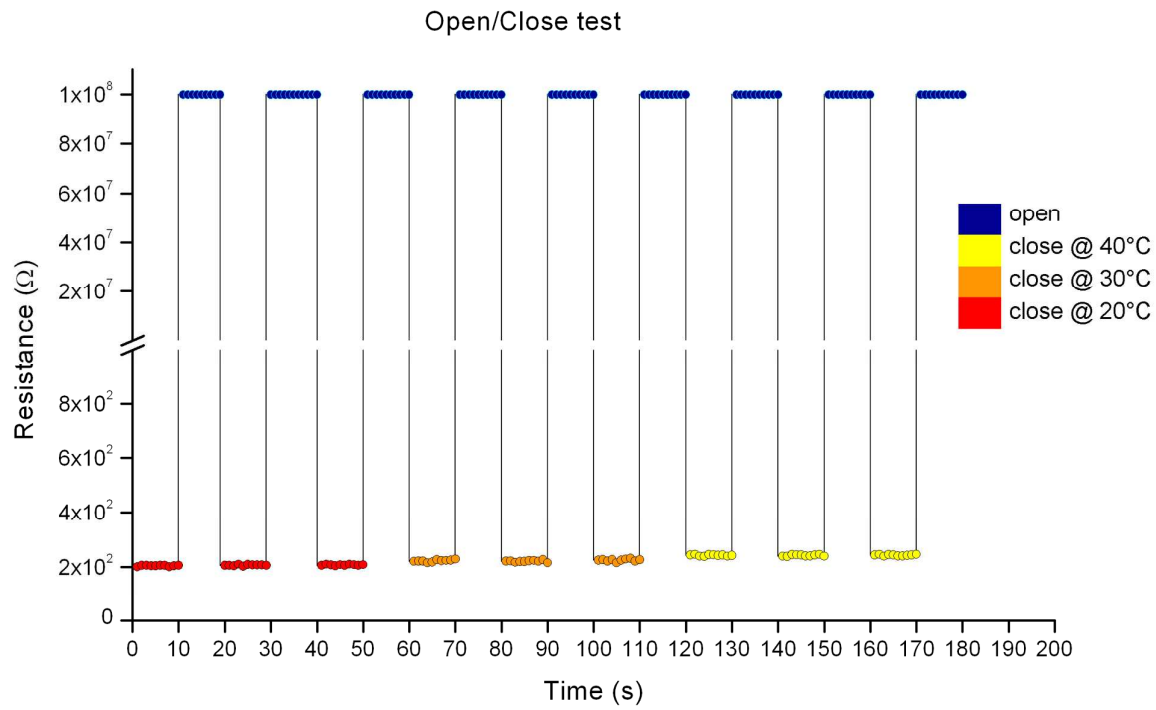Figure 4: Resistance versus temperature plots. The continuous black curve represents the cubic curve that fits the experimental data

Figure 5: open/close test at different temperatures.